Available online at www.sciencedirect.com
ScienceDirect
Journal of Sound and Vibration 323 (2009) 802–825
JOURNAL OF SOUND AND VIBRATION
www.elsevier.com/locate/jsvi

Uncertainty in structural dynamics: Experimental validation of a Wishart random matrix model

S. Adhikari[a,*,1], A. Sarkar[b,2]

[a]School of Engineering, Swansea University, Singleton Park, Swansea SA2 8PP, UK
[b]Department of Civil and Environmental Engineering, Carleton University, Ottawa, Canada

Received 24 September 2007; received in revised form 14 January 2009; accepted 15 January 2009
Handling Editor: C.L. Morfey
Available online 24 February 2009

Abstract

In the modeling of complex dynamical systems, high-resolution finite element models are routinely adopted to reduce the discretization error. Such an approach may fail to enhance the confidence in simulation-based predictions when the dynamical systems exhibit significant variability in the parameterization and description of the mathematical model due to parametric (data) uncertainty and model uncertainty. In contrast to parametric uncertainty, model uncertainty poses significant challenges as no explicit parameter is available a priori to characterize its behavior. In the current investigation, a set of sprung-mass oscillators randomly attached to a baseline system (namely, a homogeneous cantilever plate) gives rise to model uncertainty. Contrary to model parametric uncertainty traditionally tackled using stochastic finite element method (SFEM), the model uncertainty arising from randomly attached sprung-masses gives rise to a new variant of dynamical system for every sample. The feasibility of adopting a Wishart random matrix to represent such ensemble of dynamical systems derived from model perturbation is investigated in this paper. The experiments conducted on a vibrating plate with randomly attached sprung-mass oscillators demonstrate that the Wishart random matrix model may provide a reasonable representation of model uncertainty in linear dynamical systems in the medium and high-frequency region.

1. Introduction

High-resolution finite element models (FEM) are routinely adopted as predictive tools for complex dynamical systems such as aerospace, marine and automotive vehicles. Recent availability of cost-effective high-performance computing platforms offer practical means to solve such large-scale linear systems using parallel processing. Although such high-resolution numerical models can reduce discretization errors, in numerous cases, experimental results and numerical predictions exhibit significant variabilities stemming from

*Corresponding author. Tel.: +44 1792 602088; fax: +44 1792 295676.
E-mail addresses: S.Adhikari@swansea.ac.uk (S. Adhikari), abhijit_sarkar@carleton.ca (A. Sarkar).
URL: http://engweb.swan.ac.uk/~adhikaris (S. Adhikari), http://www.abhijitsarkar.net/ (A. Sarkar).
[1]Chair of Aerospace Engineering.
[2]Assistant Professor and Canada Research Chair.

0022-460X/$ - see front matter © 2009 Elsevier Ltd. All rights reserved.
doi:10.1016/j.jsv.2009.01.030

Nomenclature

$\mathbf{A}(\omega)$	dynamic stiffness matrix
$\mathbf{B}_n$	$n^2 \times n(n+1)/2$-dimensional translation matrix
$\mathbf{D}(\omega)$	dynamic stiffness matrix
$\mathbf{f}(t)$	forcing vector
$\mathbf{G}$	symbol for a system matrix, $\mathbf{G} \equiv \{\mathbf{M}, \mathbf{C}, \mathbf{K}\}$
$\mathbf{H}(\omega)$	frequency response function (FRF) matrix
$\mathbf{M}$, $\mathbf{C}$	and $\mathbf{K}$ mass, damping and stiffness matrices, respectively
n	number of degrees of freedom
$p, \mathbf{\Sigma}$	scalar and matrix parameters of the Wishart distribution
$p_{(\bullet)}(\mathbf{X})$	probability density function of $(\bullet)$ in (matrix) variable $\mathbf{X}$
$\mathbf{q}(t)$	response vector
$\mathbb{R}$	space of real numbers
$\mathbb{R}_n^+$	space $n \times n$ real positive definite matrices
$\mathbb{R}^{n\times m}$	space $n \times m$ real matrices
$\text{etr}\{\bullet\}$	$\exp\{\text{Trace}(\bullet)\}$
$\text{Trace}(\bullet)$	sum of the diagonal elements of a matrix
$(\bullet)^{\text{T}}$	matrix transposition
$\tilde{(\bullet)}$	Fourier transform of $(\bullet)$
$\lvert \bullet \rvert$	determinant of a matrix
$\lVert \bullet \rVert_{\text{F}}$	Frobenius norm of a matrix, $\lVert \bullet \rVert_{\text{F}} = (\text{Trace}((\bullet)(\bullet)^{\text{T}}))^{1/2}$
$\otimes]$	Kronecker product (see Ref. [56]
$\sim$	distributed as
$\Gamma_n(a)$	multivariate gamma function
δ_{ij}	Kronecker's delta function
v	order of the inverse-moment constraint
ω	excitation frequency
cdf	cumulative distribution function
FRF	frequency response function
pdf	probably density function
RMT	random matrix theory
SFEM	stochastic finite element method

the random scatter in model parameters and imperfect models (e.g. Ref. [1]). When substantial statistical information is available, the scatter in the model parameters can be represented using probabilistic methods. In this case one can fit probability density functions (pdf) corresponding to available data and consequently the model parameters can be expressed as random variables or random processes and the resulting problem can be solved using stochastic finite element method (SFEM) [2–15]. However, such parametric approaches may not be suitable when: (1) the parameters contributing to the modeling errors are not known a priori, (2) exceedingly large number of random variables or processes are necessary to tackle uncertainty. As a result, the representation and quantification of model uncertainty poses conceptual and computational difficulties.

Modeling of complex systems, such as the marine (e.g. ships and submarines) and aerospace systems (e.g. helicopters, aircrafts and space shuttles), modeling error arises naturally due to incomplete knowledge of the system (e.g. Refs. [16–19]). For instance, model uncertainty may manifest in the form of randomly attached subsystems to the primary structure. In certain cases, even the presence or absence of such subsystem components on the main structure may not be known precisely. For typical marine and aerospace structures, the cargo, piping, fuel, control cables, electronics and avionic systems, hydraulics and bulkheads constitute such subsystems (e.g. Ref. [17]). In the low-frequency regions, the effect of such substructure may be adequately modeled by rigid masses coupled to the primary structure (e.g. Ref. [16]). In the higher frequency regions, the mechanics of energy flow among the primary and secondary systems may not be captured by rigid masses alone as the dynamics of the subsystems become increasingly important (e.g. Ref. [16]). The additional degrees of freedom (dof) arising from the subsystems should be incorporated to simulate the entire system. For simplicity, the sprung-mass models are adopted in the current study to investigate the effect of such subsystems on the dynamics of the main structure. For numerous complex systems, the main structural parts (the primary or master structure) can often be modeled deterministically using the conventional finite element method [20]. The underlying assumption is that the constitutive and geometric properties including the boundary conditions are known with sufficient accuracy leading to a well-defined boundary value problem. On the other hand, the substructures (secondary systems) attached to the primary structure may not be practically accessible for conventional finite element modeling due to lack of detailed knowledge of such subsystems. It attributes (but not restricted) to the simplified mechanistic and statistical assumptions made due

to: (1) the lack of knowledge regarding the presence of such subsystems, (2) the lack of knowledge regarding their spatial locations with respect to the primary structure, (3) imprecise and incomplete information about their constitutive and geometric properties, (4) incompatible physical laws (demanding complex multiphysics modeling), (5) incompatible geometric scales (demanding complex multiscale modeling), (6) unknown coupling characteristics and (7) the simplified assumptions on the probability laws of the system parameters due to scarcity of measurement data.

Soize [16] introduced the concept of *fuzzy* structures to address some of these issues whereby the dynamical effect of the secondary systems are incorporated through *random* impedance functions while analyzing the entire dynamical system. In the low frequency region, characterized by predominantly modal response, the effect of such subsystems can simply be modeled by randomly distributed added masses without increasing the total number of dof. Such approach however renders ineffective in the mid-frequency range where the secondary systems act as energy sinks by absorbing energy from the primary structures (e.g. Ref. [17]). For the transient vibration, the energy stored in the secondary systems may transfer back and forth to the primary structures (e.g. Ref. [17]). For such energy transfer mechanism, it is necessary to model the subsystems by *sprung-mass systems* (instead of just pure added masses [16]). It increases the total number of dof of the complete system. By explicitly modeling the secondary systems with additional dofs not only permits the analyst to accurately estimate the amplitude of the direct- and cross-frequency response functions (FRFs), but also to predict the average phases, being significant to study wave-propagation effects.

We focus on the effect of modeling uncertainty in the primary system emerging from a set of randomly distributed sprung-masses. This may be construed to simulate the effect of *uncertain* secondary systems whose spatial attachment locations and dynamic characteristics are not available *a priori*. The model uncertainty arising from the sprung-mass oscillators generates new varieties of dynamical system for each sample as alluded previously. This can be observed from the variation in *sparsity structure* of the mass, stiffness and damping matrices of the total system from sample to sample. In this study, we investigate the feasibility of adopting a global probabilistic model to describe such ensemble of dynamical systems derived from model perturbation using random matrix theory pioneered by Soize et al. [21–30] and subsequently adopted by others [31–34]. In particular, Wishart random matrices e.g. Refs. [35,32–34] are considered as a suitable candidate for this purpose. The inverse problem involving fitting the optimal parameters of Wishart matrices representing the mass, stiffness and damping matrices are discussed. These random matrices preserve the positive-definiteness, symmetry and certain physically realistic criteria based on the baseline system. By fitting a global model, the identification of such statistical system circumvents the need of local parametrization (which may be impractical in many situations).

The few experimental studies on random systems conducted so far [36–38] do not explicitly consider model uncertainty. The experiments reported here attempt to simulate the influence of *uncertain* secondary systems on the dynamics of a thin plate (i.e. the primary structure) that gives rise to model uncertainty. A cantilever steel plate with 10 spring-mass oscillators is considered. The spatial attachment locations and the natural frequencies of the spring-mass oscillators are assumed to be random. The tests are closely controlled and the uncertainty is considered to be 'known' for validation purposes. These experiments permits us to fit Wishart random matrix model for representation of uncertainty, to propagate it through the dynamical system and to compare the results with this experimentally obtained data. One hundred nominally identical dynamical systems were created and individually tested. The experimental data presented here are available on the world wide web for research purposes. The web address is http://engweb.swan.ac.uk/~adhikaris/uq/. The outline of the paper is as follows. A brief overview of linear dynamical systems with uncertainty is discussed in Section 2. In Section 3 the concept of matrix variate distribution or random matrices is discussed. The Wishart random matrix models, its parameters and numerical simulation is discussed in Section 4. The model of the cantilever plate and the experimental setup are described in Section 5. The experimental method to test 100 nominally identical structures is discussed in Section 5.2. In Section 5.3, a Wishart random matrix model for the experimental system with random oscillators is numerically simulated using the thin plate theory and Monte Carlo simulation. In Section 6 the mean and standard deviation of the amplitude and phase of the experimentally measured FRFs are compared with random matrix simulation results. The key results and the contributions of this work are discussed in Section 7.

2. Uncertain dynamical system

The equation of motion of a damped n-degree-of-freedom linear dynamical system can be expressed as

$$\mathbf{M}\ddot{\mathbf{q}}(t) + \mathbf{C}\dot{\mathbf{q}}(t) + \mathbf{K}\mathbf{q}(t) = \mathbf{f}(t) \tag{1}$$

where $\mathbf{M} \in \mathbb{R}^{n\times n}$, $\mathbf{C} \in \mathbb{R}^{n\times n}$ and $\mathbf{K} \in \mathbb{R}^{n\times n}$ are the mass, damping and stiffness matrices, respectively. In the framework of probability theory, uncertainty in the system leads to random mass, stiffness and damping matrices. The importance of considering uncertainty largely depends on the frequency of excitation that drives the system. As the wavelengths of the vibration decreases with higher frequency, the dynamic response becomes increasingly sensitive to small details regarding the system parameters [39]. Furthermore, the dynamics of secondary systems play an important role as these subsystems can significantly affect both the amplitude and phases of the vibration. In addition, modeling uncertainty arising from the effect of unknown or imprecisely known subsystems should be considered to improve the accuracy of numerical predictions (e.g. Refs. [16,17,19,18]). The parametric approach (generally used to represent the uncertainty in the local system parameters) becomes impractical to describe the model uncertainty.

Two types of non-parametric approaches that can be used are (a) statistical energy analysis (SEA) (see for example Refs. [40,41,8,42–44]) and (b) random matrix based approach (e.g. Refs. [21–24,26,31–34]). In this paper we adopt the Wishart random matrix based approach due to the fact that uncertainty related parameters corresponding to the system matrices can be identified from experimental measurements. Some noteworthy points of this approach are:

(1) It circumvents the need for the detailed statistical characterization of local parameters—instead the statistical dispersions of global system properties (e.g. the mass, stiffness and damping matrices) are used directly.
(2) Each sample of a random system matrix is symmetric and positive-definite and thus being an appropriate model for the mass, stiffness and damping matrices of a linear self-adjoint system.
(3) The mean values of the random mass, stiffness and damping matrices are close to those of the *baseline* predictive model.
(4) A single parameter controls the statistical dispersion of each matrix. Such dispersion parameters can be estimated from experimental measurements [23,25,31]. Due to such a single parametric dependence, it is therefore difficult to match the detailed correlations structure among the elements of the system matrices when such information is indeed available.
(5) The approach can simultaneously account for parametric and model uncertainty. However, an open question still remains on the inability of the random matrix theory to consider the statistical correlations among the mass, stiffness and damping matrices as well as accounting the correlations among the elements of each of these matrices.

In general, the mass, stiffness and damping matrices arising in FEM model exhibit well-defined banded structures under the assumption that the geometrical configuration and constitutive properties of the system are perfectly known. In reality, there may be random errors in the specifications of the geometry. For example, consider two plates connected an exact right angle (which will be considered as the perfect system). Due to slight misalignment in the right angled connection, the resulting imperfect system matrices will have different sparsity structure compared to the perfect system. Such uncertainty in the specification of geometry induces randomness in the sparsity pattern of the FEM system matrices. Another case of difference in the sparsity structure has been recently reported [45–47] in the context of finite element modeling of systems with non-local damping and stiffness properties. If there are uncertainties associated with non-locality in the damping and stiffness properties in some part of a complex structure, it would result in randomness in the sparsity of the mass, stiffness and damping matrices of the system. This situation may arise in the use of advanced composite or damping material in some part of a system. The parametric uncertainty quantification methods experience difficulty (1) to tackle model uncertainty, and (2) to handle an exceedingly large number of random parameters necessary to model uncertainty. These difficulties lead us to consider the possibility of using the alternative approach based on random matrix theory as detailed next.

3. Matrix variate distributions

We are primarily interested to investigate feasible alternatives to tackle uncertainties whose treatment in the framework of conventional parametric method is not practicable. For example, one may consider the case when exceedingly large numbers of random parameters are necessary to describe uncertainty under *sparse* statistical information. This has prompted us to consider matrix variate distribution to model system matrices. Matrix variate pdf can be used to completely define a random matrix (as a univariate pdf completely defines a random variable). A random matrix can be considered as an observable phenomenon representable in the form of a matrix which under repeated observation yields different non-deterministic outcomes. The pdf of a random matrix can be defined in a manner similar to that of a random variable or random vector. If $\mathbf{A}$ is an $n \times m$ real random matrix, the matrix variate pdf of $\mathbf{A} \in \mathbb{R}^{n\times m}$, denoted by $p_{\mathbf{A}}(\mathbf{A})$, is a mapping from the space of $n \times m$ real matrices to the real line, i.e., $p_{\mathbf{A}}(\mathbf{A}) : \mathbb{R}^{n\times m} \to \mathbb{R}$. Here we define the pdf of a few random matrices that are relevant to stochastic mechanics.

Gaussian random matrix: A rectangular random matrix $\mathbf{X} \in \mathbb{R}^{n\times p}$ is said to have a matrix variate Gaussian distribution with the mean matrix $\mathscr{M} \in \mathbb{R}^{n\times p}$ and the covariance matrix $\mathbf{\Sigma} \otimes \mathbf{\Psi}$, where $\mathbf{\Sigma} \in \mathbb{R}^{n}_{+}$ and $\mathbf{\Psi} \in \mathbb{R}^{p}_{+}$ provided the pdf of $\mathbf{X}$ is given by

$$p_{\mathbf{X}}(\mathbf{X}) = (2\pi)^{-np/2}|\mathbf{\Sigma}|^{-p/2}|\mathbf{\Psi}|^{-n/2}\mathrm{etr}\{-\tfrac{1}{2}\mathbf{\Sigma}^{-1}(\mathbf{X}-\mathscr{M})\mathbf{\Psi}^{-1}(\mathbf{X}-\mathscr{M})^{\mathrm{T}}\} \tag{2}$$

This distribution is usually denoted as $\mathbf{X} \sim N_{n,p}(\mathscr{M}, \mathbf{\Sigma} \otimes \mathbf{\Psi})$

Symmetric Gaussian random matrix: Let $\mathbf{Y} \in \mathbb{R}^{n\times n}$ be a symmetric random matrix and $\mathscr{M}, \mathbf{\Sigma}$ and $\mathbf{\Psi}$ are $n \times n$ matrices such that the commutative relation $\mathbf{\Sigma\Psi} = \mathbf{\Psi\Sigma}$ holds. If the $n(n+1)/2 \times 1$ vector $\mathrm{vecp}(\mathbf{Y})$ formed from $\mathbf{Y}$ is distributed as $N_{n(n+1)/2,1}(\mathrm{vecp}(\mathscr{M}), \mathbf{B}_n^{\mathrm{T}}(\mathbf{\Sigma} \otimes \mathbf{\Psi})\mathbf{B}_n)$, then $\mathbf{Y}$ is said to have a symmetric matrix variate Gaussian distribution with mean $\mathscr{M}$ and covariance matrix $\mathbf{B}_n^{\mathrm{T}}(\mathbf{\Sigma} \otimes \mathbf{\Psi})\mathbf{B}_n$ and its pdf is given by

$$p_{\mathbf{Y}}(\mathbf{Y}) = (2\pi)^{-n(n+1)/4}|\mathbf{B}_n^{\mathrm{T}}(\mathbf{\Sigma} \otimes \mathbf{\Psi})\mathbf{B}_n|^{-1/2}\mathrm{etr}\{-\tfrac{1}{2}\mathbf{\Sigma}^{-1}(\mathbf{Y}-\mathscr{M})\mathbf{\Psi}^{-1}(\mathbf{Y}-\mathscr{M})^{\mathrm{T}}\} \tag{3}$$

This distribution is usually denoted as $\mathbf{Y} = \mathbf{Y}^{\mathrm{T}} \sim SN_{n,n}(\mathscr{M}, \mathbf{B}_n^{\mathrm{T}}(\mathbf{\Sigma} \otimes \mathbf{\Psi})\mathbf{B}_n)$

For a symmetric matrix $\mathbf{Y} \in \mathbb{R}^{n\times n}$, $\mathrm{vecp}(\mathbf{Y})$ is a $n(n+1)/2$-dimensional column vector formed from the elements above and including the diagonal of $\mathbf{Y}$ taken columnwise. The elements of the translation matrix $\mathbf{B}_n \in \mathbb{R}^{n^2\times n(n+1)/2}$ are given by

$$(B_n)_{ij,gh} = \tfrac{1}{2}(\delta_{ig}\delta_{jh} + \delta_{ih}\delta_{jg}), \quad i \leqslant n,\ j \leqslant n,\ g \leqslant h \leqslant n \tag{4}$$

where δ_{ij} is the usual Kronecker's delta.

Wishart matrix: A $n \times n$ symmetric positive definite random matrix $\mathbf{S}$ is said to have a Wishart distribution with parameters $p \geqslant n$ and $\mathbf{\Sigma} \in \mathbb{R}^{n}_{+}$, if its pdf is given by

$$p_{\mathbf{S}}(\mathbf{S}) = \{2^{(1/2)np}\,\Gamma_n(\tfrac{1}{2}p)|\mathbf{\Sigma}|^{(1/2)p}\}^{-1}|\mathbf{S}|^{(1/2)(p-n-1)}\mathrm{etr}\{-\tfrac{1}{2}\mathbf{\Sigma}^{-1}\mathbf{S}\} \tag{5}$$

This distribution is usually denoted as $\mathbf{S} \sim W_n(p, \mathbf{\Sigma})$. Wishart random matrices are the simplest random matrix model for linear structural dynamics. Using a least-square error minimization approach, Adhikari [32,34] obtained the parameters of the Wishart distribution.

Matrix variate gamma distribution: A $n \times n$ symmetric positive definite random matrix $\mathbf{W}$ is said to have a matrix variate gamma distribution with parameters a and $\mathbf{\Psi} \in \mathbb{R}^{+}_{n}$, if its pdf is given by

$$p_{\mathbf{W}}(\mathbf{W}) = \{\Gamma_n(a)|\mathbf{\Psi}|^{-a}\}^{-1}|\mathbf{W}|^{a-(1/2)(n+1)}\mathrm{etr}\{-\mathbf{\Psi W}\}, \quad \Re(a) > \tfrac{1}{2}(n-1) \tag{6}$$

This distribution is usually denoted as $\mathbf{W} \sim G_n(a, \mathbf{\Psi})$. The matrix variate gamma distribution was used by Ref. [21,22] for the random system matrices of linear dynamical systems. Comparing this distribution with the Wishart distribution, we have $G_n(a, \mathbf{\Psi}) = W_n(2a, \mathbf{\Psi}^{-1}/2)$. The main difference between the gamma and the Wishart distribution is that originally only integer values were considered for the shape parameter p in the Wishart distribution. However, p is not limited to an integer number. In fact, one can easily observe that Eq. (5) is valid for all real p greater than n.

In Eqs. (5) and (6), the function $\Gamma_n(a)$ is the multivariate gamma function, which can be expressed in terms of products of the univariate gamma functions as

$$\Gamma_n(a) = \pi^{(1/4)n(n-1)} \prod_{k=1}^{n} \Gamma\left[a - \frac{1}{2}(k-1)\right] \quad \text{for } \Re(a) > \frac{1}{2}(n-1) \tag{7}$$

For more details on the matrix variate distributions we refer to the books by Tulino and Verdú [48], Gupta and Nagar [35], Eaton [49], Muirhead [50], Girko [51] and references therein. Among the three types of random matrices introduced above, the distribution given by Eq. (5) will always result in symmetric and positive definite matrices. Therefore, it can be a possible candidate for modeling random system matrices arising in probabilistic structural mechanics.

4. Wishart random matrices in structural dynamics

4.1. Parameters of Wishart random matrices

Suppose that $\overline{\mathbf{M}}$, $\overline{\mathbf{C}}$ and $\overline{\mathbf{K}}$ are, respectively, the mass, damping and stiffness matrices corresponding to the baseline system. This information is likely to be available, for example, using the deterministic finite element method in conjunction with modal updating [52]. However, there are uncertainties associated with our modeling so that $\mathbf{M}$, $\mathbf{C}$ and $\mathbf{K}$ are actually random matrices whenever a probabilistic approach is adopted. The matrices $\overline{\mathbf{M}}$, $\overline{\mathbf{C}}$ and $\overline{\mathbf{K}}$ are the best known information regarding the system matrices and may be close to the mean of the underlying random matrix ensemble of $\mathbf{M}$, $\mathbf{C}$ and $\mathbf{K}$. The matrix variate distributions of the random system matrices should be such that [21–24,26,31–34]: (1) $\mathbf{M}$, $\mathbf{C}$ and $\mathbf{K}$ are symmetric matrices, (2) $\mathbf{M}$ is positive-definite and $\mathbf{C}$ and $\mathbf{K}$ are non-negative-definite matrices, and (3) the moments of the inverse of the dynamic stiffness matrix

$$\mathbf{D}(\omega) = -\omega^2\mathbf{M} + \mathrm{i}\omega\mathbf{C} + \mathbf{K} \tag{8}$$

should exist $\forall\omega$. That is, if $\mathbf{H}(\omega)$ is the FRF matrix, given by

$$\mathbf{H}(\omega) = \mathbf{D}^{-1}(\omega) = [-\omega^2\mathbf{M} + \mathrm{i}\omega\mathbf{C} + \mathbf{K}]^{-1} \tag{9}$$

the following condition must be satisfied:

$$\mathrm{E}[\|\mathbf{H}(\omega)\|_{\mathrm{F}}^{v}] < \infty, \quad \forall\omega \tag{10}$$

Here v is the order of the inverse-moment constraint. For example if $\mathbf{H}(\omega)$ is considered to be a second-order (matrix variate) random process then $v = 2$ should be used. This constraint is clearly arising from the fact that the moments and the pdf of the response vector must exist for all frequency of excitation. Because the matrices $\mathbf{M}$, $\mathbf{C}$ and $\mathbf{K}$ have similar probabilistic characteristics, for notational convenience we will use the notation $\mathbf{G}$ which stands for any one of the system matrices. Suppose the matrix variate density function of $\mathbf{G} \in \mathbb{R}_n^+$ is given by $p_{\mathbf{G}}(\mathbf{G}) : \mathbb{R}_n^+ \to \mathbb{R}$. We have the following information and constrains to obtain $p_{\mathbf{G}}(\mathbf{G})$:

$$\int_{\mathbf{G}>0} p_{\mathbf{G}}(\mathbf{G})\,\mathrm{d}\mathbf{G} = 1 \quad \text{(the normalization)} \tag{11}$$

and

$$\mathrm{E}[\mathbf{G}] = \int_{\mathbf{G}>0} \mathbf{G}\,p_{\mathbf{G}}(\mathbf{G})\,\mathrm{d}\mathbf{G} = \overline{\mathbf{G}} \quad \text{(the mean matrix)} \tag{12}$$

The mean matrix $\overline{\mathbf{G}}$ is symmetric and positive definite and the integrals appearing in these equations are $n(n+1)/2$ dimensional.

The exact application of the constraint that the inverse-moments of the dynamic stiffness matrix should exist for all frequencies requires the derivation of the joint pdf of the random matrices $\mathbf{M}$, $\mathbf{C}$ and $\mathbf{K}$. Instead of dealing with the complex dynamic stiffness matrix, we consider a simpler problem where it is required that the inverse moments of each of the system matrices $\mathbf{M}$, $\mathbf{C}$ and $\mathbf{K}$ must exist. Provided the system is damped, this condition will always guarantee the existence of the moments of the FRF matrix. This is only a *sufficient condition* and not

a necessary condition. As a result, except the stiffness matrix (to take account of the static case when $\omega = 0$), the distributions arising from this approach will be more constrained than that is necessary.

Maximizing the entropy associated with the matrix variate pdf $p_{\mathbf{G}}(\mathbf{G})$

$$\mathscr{S}(p_{\mathbf{G}}) = -\int_{\mathbf{G}>0} p_{\mathbf{G}}(\mathbf{G}) \ln\{p_{\mathbf{G}}(\mathbf{G})\}\, \mathrm{d}\mathbf{G} \tag{13}$$

and using the constraints in Eqs. (11) and (12) Soize [21,22,24] proved that the system matrices should follow the matrix variate Gamma distribution, which in turn is related to the Wishart distribution as $W_n(p,\boldsymbol{\Sigma}) = G_n(p/2, \frac{1}{2}\boldsymbol{\Sigma}^{-1})$. In particular it was shown that the maximum-entropy pdf of $\mathbf{G}$ follows the Wishart distribution with parameters $p = (2v + n + 1)$ and $\boldsymbol{\Sigma} = \overline{\mathbf{G}}/(2v + n + 1)$, that is $\mathbf{G} \sim W_n(2v + n + 1, \overline{\mathbf{G}}/(2v + n + 1))$.

It was later observed that [32] with this distribution, there can be significant discrepancy between the 'mean of the inverse' and the 'inverse of the mean' of a system matrix. To overcome this problem, using a least-square error minimization approach, Adhikari [32] proposed the optimal distribution of $\mathbf{G}$. This is given by $\mathbf{G} \sim W_n(p, \boldsymbol{\Sigma})$, where

$$p = n + 1 + \theta_G \tag{14}$$

and

$$\boldsymbol{\Sigma} = \overline{\mathbf{G}}/\alpha_G \tag{15}$$

The constants θ_G and α_G are obtained as

$$\theta_G = \frac{1}{\sigma_G^2}\left\{1 + \frac{\{\mathrm{Trace}(\overline{\mathbf{G}})\}^2}{\mathrm{Trace}(\overline{\mathbf{G}}^2)}\right\} - (n+1) \tag{16}$$

and

$$\alpha_G = \sqrt{\theta_G(n + 1 + \theta_G)} \tag{17}$$

Here σ_G is known as the dispersion parameter which characterizes the uncertainty in the random matrix $\mathbf{G}$. The parameter σ_G is defined as

$$\sigma_G^2 = \frac{\mathrm{E}[\|\mathbf{G} - \mathrm{E}[\mathbf{G}]\|_{\mathrm{F}}^2]}{\|\mathrm{E}[\mathbf{G}]\|_{\mathrm{F}}^2} \tag{18}$$

From this expression observe that σ_G can be viewed as the mean-normalized standard deviation of the random matrix $\mathbf{G}$. The first moment (mean) and the elements of the covariance tensor is given by [35]

$$\mathrm{E}[\mathbf{G}] = p\boldsymbol{\Sigma} = p\overline{\mathbf{G}}/\alpha_G \tag{19}$$

$$\mathrm{cov}(G_{ij}, G_{kl}) = p(\Sigma_{ik}\Sigma_{jl} + \Sigma_{il}\Sigma_{jk}) = \frac{1}{\theta_G}(\overline{G}_{ik}\overline{G}_{jl} + \overline{G}_{il}\overline{G}_{jk}) \tag{20}$$

In Eq. (20), note that the values of $\overline{G}_{ik}$ are fixed by the mean matrix. Therefore, the *only* parameter that controls the uncertainty in the distribution is θ_G. The value of θ_G should be calculated from σ_G by Eq. (16). The parameter σ_G contains the information regarding the model uncertainty which needs to be obtained from physical or computer experiments.

In a recent work [34] following four different approaches are compared to identify the parameters of Wishart distribution:

- Approach 1, Soize [21,22,24]: The mean of the random matrix is same as the deterministic matrix and the normalized standard deviation is same as the measured normalized standard deviation.
- Approach 2, Adhikari [32]: The mean of the random matrix and the mean of the inverse of the random matrix are closest to the deterministic matrix and its inverse.
- Approach 3, Adhikari [34]: The mean of the inverse of the random matrix equals to the inverse of the deterministic matrix and the normalized standard deviation is same as the measured normalized standard

deviation. For this condition one obtains

$$p = n + 1 + \theta_G \quad \text{and} \quad \boldsymbol{\Sigma} = \overline{\mathbf{G}}/\theta_G \tag{21}$$

where θ_G is defined in Eq. (16).

- Approach 4, Adhikari [34]: The mean of the eigenvalues of the distribution is same as the 'measured' eigenvalues of the mean matrix and the normalized standard deviation is same as the measured normalized standard deviation.

It is shown that approach 3 [34], that is when the mean of the inverse equals to the inverse of the mean of the system matrices, the calculated response statistics are in best agreements with the direct numerical simulation results. As a result we will use the parameters corresponding to Eq. (21) for the Wishart matrices.

4.2. Monte Carlo simulation of Wishart matrices

As discussed in the previous subsection, for all practical purposes the random matrix model for a system matrix can be considered Wishart matrix with parameters $p = n + 1 + \theta$ and $\boldsymbol{\Sigma} = \overline{\mathbf{G}}/\theta$. This leads to a simple and general simulation algorithm for probabilistic structural dynamics. The method can be implemented according to the following steps:

(1) Form the deterministic matrices $\overline{\mathbf{G}} \equiv \{\overline{\mathbf{M}}, \overline{\mathbf{C}}, \overline{\mathbf{K}}\}$ using the standard finite element method. Obtain n, the dimension of the system matrices.
(2) Obtain the normalized standard deviations or the dispersion parameters $\sigma_G \equiv \{\sigma_M, \sigma_C, \sigma_K\}$ corresponding to the system matrices. This can be obtained from physical or computer experiments. This is the *only* information regarding the system uncertainty that is required in this approach.
(3) Calculate

$$\theta_G = \frac{1}{\sigma_G^2}\left\{1 + \frac{\{\text{Trace}(\overline{\mathbf{G}})\}^2}{\text{Trace}(\overline{\mathbf{G}}^2)}\right\} - (n+1) \quad \text{for } \mathbf{G} = \{\mathbf{M}, \mathbf{C}, \mathbf{K}\} \tag{22}$$

(4) Approximate $(n + 1 + \theta_G)$ to its nearest integer and call it p. That is $p = [n + 1 + \theta_G]$. For complex engineering systems n can be in order of several thousands or even millions. As shown in the numerical example before, this approximation would introduce negligible error. Create a $n \times p$ matrix $\widetilde{\mathbf{X}}$ with Gaussian random numbers with zero mean and unit covariance i.e., $\widetilde{\mathbf{X}} \sim N_{n,p}(\mathbf{O}, \mathbf{I}_n \otimes \mathbf{I}_p)$.
(5) Because $\boldsymbol{\Sigma} = \overline{\mathbf{G}}/\theta_G$ is a positive definite matrix, it can be factorized as $\boldsymbol{\Sigma} = \boldsymbol{\Gamma}\boldsymbol{\Gamma}^{\mathrm{T}}$. Using the matrix $\boldsymbol{\Gamma} \in \mathbb{R}^{n \times n}$, obtain the matrix $\mathbf{X}$ using the linear transformation

$$\mathbf{X} = \boldsymbol{\Gamma}\widetilde{\mathbf{X}} \tag{23}$$

Following theorem 2.3.10 in Ref. [35] it can be shown that $\mathbf{X} \sim N_{n,p}(\mathbf{O}, \boldsymbol{\Sigma} \otimes \mathbf{I}_p)$.
(6) Now obtain the samples of the Wishart random matrices $W_n(n + 1 + \theta_G, \overline{\mathbf{G}}/\theta_G)$ as

$$\mathbf{G} = \mathbf{X}\mathbf{X}^{\mathrm{T}} \tag{24}$$

Alternatively, MATLAB® command `wishrnd` can be used to generate the samples of Wishart matrices. MATLAB® can handle fractional values of $(n + 1 + \theta_G)$ so that the approximation to its nearest integer in step 5 may be avoided.
(7) Repeat the above process for the mass, stiffness and damping matrices and solve the equation of motion for each sample to obtain the response statistics of interest.

The above procedure can be implemented very easily. Once the samples of the system matrices are generated, the rest of the analysis is identical to any Monte Carlo simulation based approach. If one implements this approach in conjunction with a commercial finite element software, the commercial software needs to be accessed only once to obtain the mean matrices. This simulation procedure is 'non-intrusive'.

5. A plate with disorderly attached sprung-mass oscillators

In this section, we consider the dynamics of a steel cantilever plate with homogeneous geometric (i.e. uniform thickness) and constitutive properties (i.e. uniform Young's modulus and Poisson's ratio). This uniform plate defines our *baseline* system. The baseline model is perturbed by a set of sprung-mass oscillators, each having a random natural frequency and attached randomly along the plate. Due to sprung-mass oscillators, the uncertainty in the system therefore appears concurrently both in spatial and frequency domain. When only limited statistical information is available, it is difficult to model such complex uncertainty in terms of random variables and stochastic processes, especially when the number of such random oscillators is too large. This fact prompted us to investigate the feasibility of adopting random matrix theory to describe such uncertainty.

5.1. Model description

The uncertain dynamics is realized by 10 sprung-mass oscillators with randomly distributed stiffness properties attached at random locations. This test rig has been designed for simplicity, ease of replication and modeling. The overall arrangement of the test-rig is shown in Fig. 1.

A rectangular steel plate with uniform thickness is used for the experiment. The physical and geometrical properties of the steel plate are shown in Table 1.

Fig. 1. The test rig for the cantilever plate: (a) front view of the experimental setup and (b) side view of the experimental setup.

The plate is clamped along one edge using a clamping device. The clamping device is attached to the top of a heavy concrete block and the entire assembly is placed on a steel table. The plate has a mass of approximately 12.47 kg and special care has been taken to ensure its stability and to minimize vibration transmission. The plate is 'divided' into 375 elements (25 along the length and 15 along the width). Taking one corner of the cantilevered edge as the origin, coordinates have been assigned to all of the nodes. The oscillators and accelerometers are attached to these nodes. This approach allows straightforward correlation to a FEM, to which the oscillators are attached and the measurements are made at the nodes of the model. The bottom surface of the plate is marked with the node numbers so that the oscillators can be hung at the nodal locations.

Table 1
Material and geometric properties of the cantilever plate considered for the experiment.

Plate properties	Numerical values
Length (L_x)	998 mm
Width (L_y)	530 mm
Thickness (t_h)	3.0 mm
Mass density (ρ)	7860 kg/m^3
Young's modulus (E)	2.0×10^5 MPa
Poisson's ratio (μ)	0.3
Total weight	12.47 kg

Fig. 2. Details of a typical oscillator used to simulate unmodeled dynamics. Fixed mass (magnet) 2 g, oscillatory mass (the bolt) 121.4 g. The oscillatory mass is about 1% of the total mass of the plate. The spring stiffness varies between 1.5 and 2.4×10^4 N/m.

This scheme reduces uncertainty due to measuring attachment locations of the oscillators. A discrete random number generator is used to generate the X and Y coordinates for the attachment of the oscillators. In total, 10 oscillators are used to simulate model uncertainty. The details of a typical oscillator are shown in Fig. 2.

The springs are adhesively bonded to a magnet at the top and a mass at the bottom. The magnet at the top of the assembly allows the oscillators to be easily attached to the bottom of the plate. It should be noted that the mass of the magnets would have the 'fixed mass effect'. The stiffness values of 10 springs used in the experiments are given in Table 2. This table also shows the natural frequency of the individual oscillators.

The mass of each of the 10 oscillators is 121.4 g, and hence the total oscillator mass is 1.214 kg, which is 9.8% of the mass of the plate. The springs are attached to the plate at the pre-generated nodal locations using small magnets. The small magnets (weighting 2 g) are found to be strong enough to hold the mass over the frequency range considered. A sample realization of the attached oscillators is shown in Fig. 3.

One hundred realizations of the plate coupled with sprung-mass oscillators are created by hanging the oscillators at random locations. Each realization is then individually tested in this experiment.

5.2. Experimental methodology

Experimental modal analysis [53–55] is used in this work. The three main components of the implemented experimental technique are (a) the excitation of the structure, (b) the sensing of the response, and (c) the data

Table 2
The spring stiffnesses and natural frequencies of the oscillators used to simulate model uncertainty (the mass of the each oscillator is 121.4 g).

Oscillator number	Spring stiffness ($\times 10^4$ N/m)	Natural frequency (Hz)
1	1.6800	59.2060
2	0.9100	43.5744
3	1.7030	59.6099
4	2.4000	70.7647
5	1.5670	57.1801
6	2.2880	69.0938
7	1.7030	59.6099
8	2.2880	69.0938
9	2.1360	66.7592
10	1.9800	64.2752

Fig. 3. Attached oscillators at random locations. The spring stiffness varies so that the oscillator frequencies are between 43 and 70 Hz.

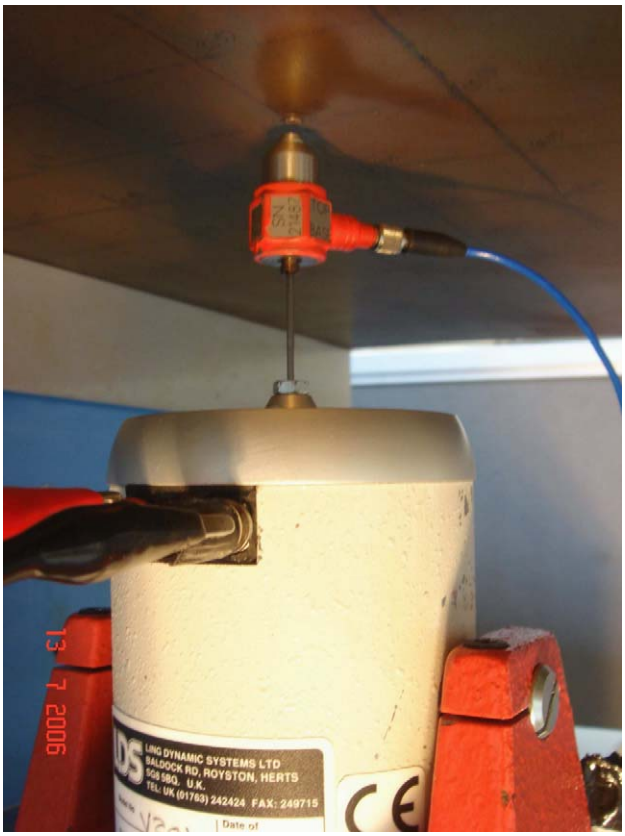

Fig. 4. The shaker used to provide an impulse excitation using Simulink™ and dSpace™. A hard steel tip was used and the shaker was placed at node (4, 6).

acquisition and processing. In this experiment a shaker was used (the make, model no. and serial no. are LDS, V201, and 92 358.3, respectively) to act as an impulse hammer. The usual manual impact hammer was not used because of the difficulty in ensuring that the impact occurs at exactly the same location with the same force for every sample run. The shaker generates impulses at a pulse interval of 20 s and a pulse width of 0.01 s. Using the shaker in this way eliminates, as far as possible, any uncertainties arising from the input forces. This innovative experimental technique is designed to ensure that the resulting uncertainty in the response arises purely due to the random locations of the attached masses. Fig. 4 shows the arrangement of the shaker.

The shaker was placed so that it impacted at the (4, 6) node of the plate. The shaker was driven by a signal from a Simulink™ and dSpace™ system via a power amplifier (TPO 25 AEI 00051). A hard steel tip is used for the hammer to increase the frequency range of excitation.

Six accelerometers are used as the response sensors. The locations of the six sensors are selected such that they cover a broad area of the plate. The locations of the accelerometers are shown in Fig. 5.

The details of the accelerometers, including their nodal locations, are shown in Table 3.

Small holes are drilled into the plate and all of the six accelerometers are attached by bolts through the holes.

The signal from the force transducer is amplified using a KISTLER type 5134 amplifier (with settings Gain: 100, Filter: 10 K and Bias: Off) while the signals from the accelerometers are directly input into the LMS system. For data acquisition and processing, LMS Test Lab 5.0 is used. In Impact Scope, the bandwidth was set to 8192 Hz with 8192 spectral lines (i.e., 1.00 Hz resolution). Five averages are taken for all of the six FRF measurements. In total $8192 \times 6 \times 101$ complex FRF data sets are stored in 101 indexed files. The data presented here are available on the world wide web for research purposes. The web address

Fig. 5. The positions of the accelerometers on the plate.

Table 3
The details of the six accelerometers attached to the top of the plate.

Model and serial number	Coordinates	LMS channel	Sensitivity (mV/g)
333M07 SN 25948	Point 1: (4, 6)	1	98.8
333M07 SN 26254	Point 2: (6, 11)	2	96.7
333M07 SN 26018	Point 3: (11, 3)	3	101.2
333M07 SN 25942	Point 4: (14, 14)	4	97.6
333M07 SN 26280	Point 5: (18, 2)	5	101.3
333M07 SN 26016	Point 6: (21, 10)	6	100.0

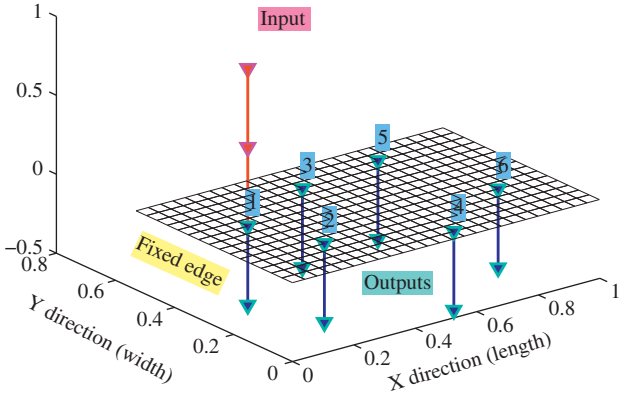

Fig. 6. The finite element (FE) model of a steel cantilever plate: 25 × 15 elements, 416 nodes, 1200 degrees-of-freedom. The material and geometric properties are: $E = 200 \times 10^9\ \mathrm{N/m^2}$, $\mu = 0.3$, $\rho = 7860\ \mathrm{kg/m^3}$, $t_h = 3.0\ \mathrm{mm}$, $L_x = 0.998\ \mathrm{m}$, $L_y = 0.53\ \mathrm{m}$. Input node number: 481, output node numbers: 481, 877, 268, 1135, 211 and 844, 0.7% modal damping is assumed for all modes.

is http://engweb.swan.ac.uk/~adhikaris/uq/. The steel tip used in the experiment only gives clean data up to approximately 4500 Hz. Therefore, 4000 Hz was used as the upper limit of the frequency in the measured FRFs. The data logged beyond 4000 Hz have been ignored for this experiment.

5.3. Numerical implementation of the random matrix approach

In this section we numerically simulate the random matrices corresponding to the experimental system discussed in Section 5.1. The objective is to determine whether the pattern of uncertainty in the experimental

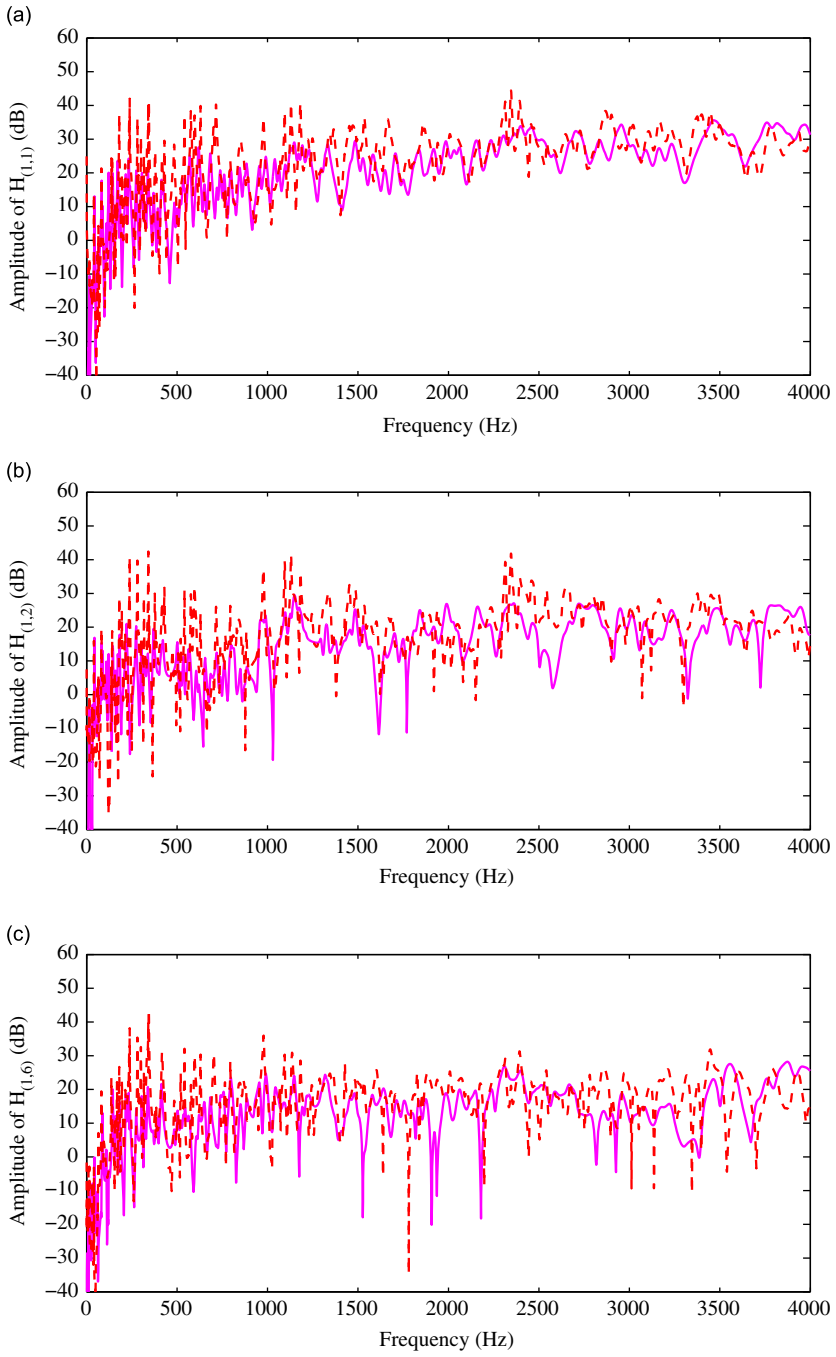

Fig. 7. Comparison of the amplitude of the FRF of the baseline system for the three selected points in the plate across the complete frequency range; – FE model; - - - experiment. (a) Driving-point FRF of the plate at point 1 (nodal coordinate: (4, 6)), (b) near-field cross-FRF of the plate at point 2 (nodal coordinate: (6, 11)), (c) far-field cross-FRF of the plate at point 6 (nodal coordinate: (21, 10)).

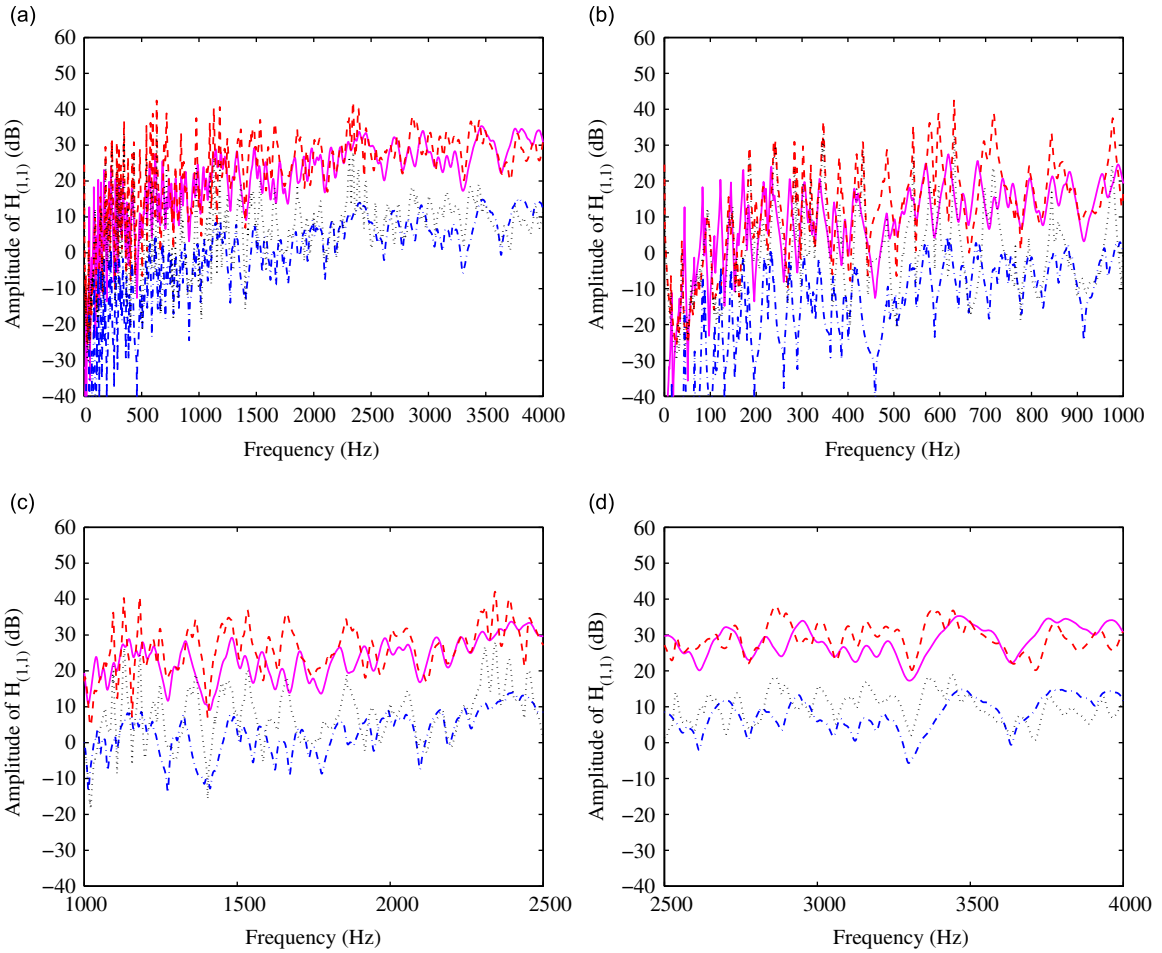

Fig. 8. Comparison of the mean and standard deviation of the amplitude of the driving-point FRF of the plate at point 1 (nodal coordinate: (4, 6)) with 10 randomly placed oscillators; — ensemble mean from Wishart model; - - - ensemble mean from experiment; -.-. standard deviation from Wishart model; … standard deviation from experiment. (a) Response across the frequency range, (b) low-frequency response, (c) medium-frequency response, (d) high-frequency response.

data can be described using the random matrix approach. A steel cantilever plate with homogeneous geometric (i.e. uniform thickness) and constitutive properties (i.e. uniform Young's modulus and Poisson's ratio) was considered. The numerical values of the material properties are given in Table 1. This uniform plate simulates the *baseline* system shown in Fig. 1. The diagram of the plate together with its numerical details is shown in Fig. 6. The plate is excited by a unit harmonic force and the responses are calculated at the points shown in the diagram.

The input node corresponds to the location of the shaker shown in Fig. 4 and the output nodes relate to the locations of the accelerometers shown in Fig. 5. In the numerical calculations 375 elements are used and the resulting FEM has 1200 dof. Only the first 280 modes (which is slightly over 4 kHz) are used in calculating the FRFs.

A modal damping factor of 0.7% is assumed for all of the modes. A constant damping factor for all the modes is an assumption. Ideally one should identify modal damping factors for all possible modes and perhaps take an average over the 100 realizations in the experiment. It is, however, a widely established practice to treat damping in a simple manner such as a constant modal damping factor as considered here. This study also verifies if such ad hoc assumptions on damping can produce any meaningful predictions.

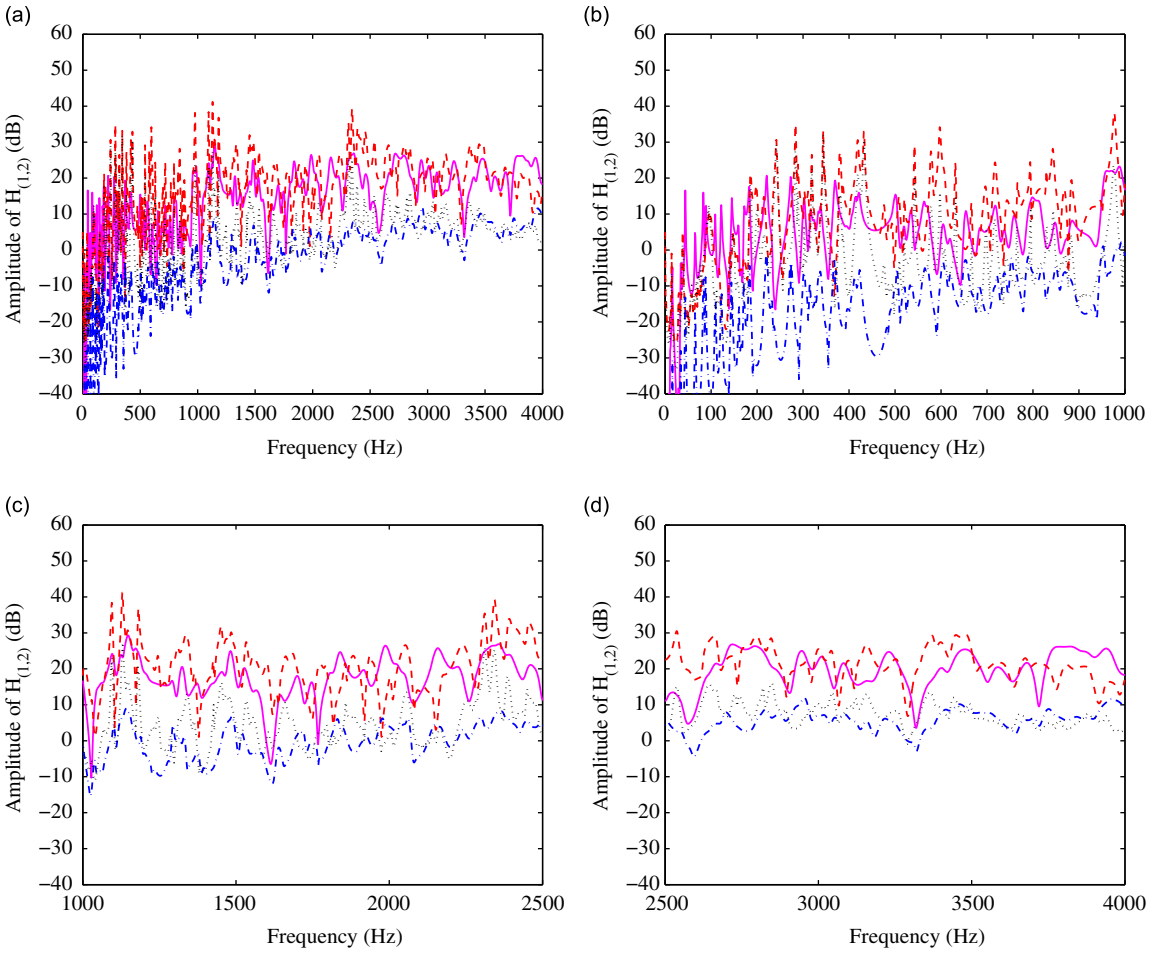

Fig. 9. Comparison of the mean and standard deviation of the amplitude of the near-field cross-FRF of the plate at point 2 (nodal coordinate: (6, 11)) with 10 randomly placed oscillators; – ensemble mean from Wishart model; - - - ensemble mean from experiment; -.-. standard deviation from Wishart model; ... standard deviation from experiment. (a) Response across the frequency range, (b) low-frequency response, (c) medium-frequency response, (d) high-frequency response.

Two key parameters are needed to implement the random matrix approach. They are, respectively, the mean and normalized standard deviation of the system matrices. The mean system is considered to be the cantilever plate shown in Fig. 6. The mean mass and stiffness matrices are obtained using the standard finite element approach. The mean damping matrix for the experimental system is not obtained explicitly as constant modal damping factors are used. All 100 realizations of the plate and oscillators were individually simulated. Then the samples of 1200×1200 mass and stiffness matrices were stored. Normalized standard deviation of the mass and stiffness matrices are obtained using Eq. (18) as $\sigma_M = 0.0286$ and $\sigma_K = 0.0017$. Since 0.7% constant modal damping factor is assumed for all the modes, $\sigma_C = 0$. The *only* uncertainty related information used in the random matrix approach are the values of σ_M and σ_K. The explicit information regarding the spatial locations of the attached oscillators including their stiffness and mass properties are *not* used in fitting the Wishart matrices. This is aimed to depict a realistic situation when the detailed information regarding uncertainties in a complex engineering system is not available to the analyst. Using $n = 1200$, $\sigma_M = 0.0286$ and $\sigma_K = 0.0017$, together with the deterministic values of $\mathbf{M}$ and $\mathbf{K}$ we obtain

$$\theta_M = 416\,437 \quad \text{and} \quad \theta_K = 116\,161\,959. \tag{25}$$

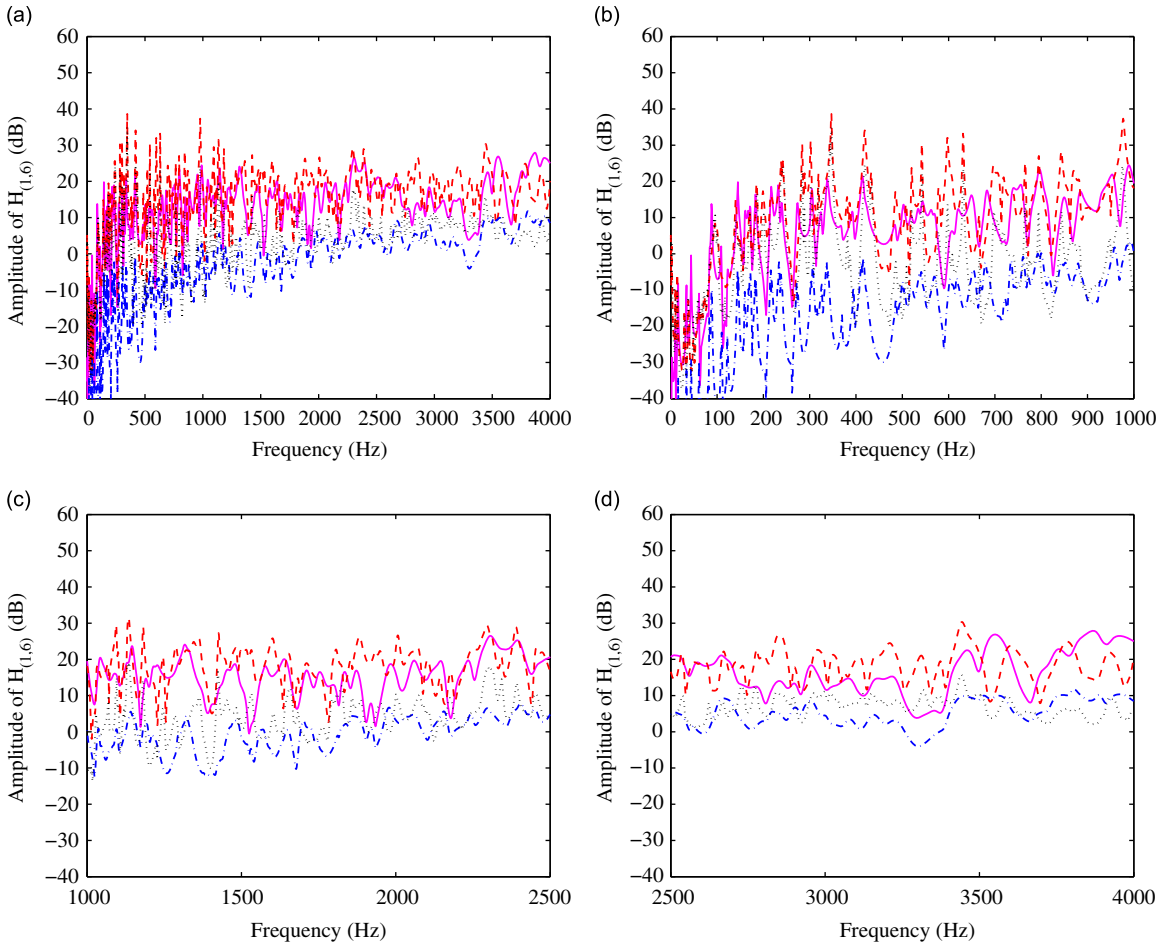

Fig. 10. Comparison of the mean and standard deviation of the amplitude of the far-field cross-FRF of the plate at point 6 (nodal coordinate: (21, 10)) with 10 randomly placed oscillators; — ensemble mean from Wishart model; - - - ensemble mean from experiment; -.-. standard deviation from Wishart model; ... standard deviation from experiment. (a) Response across the frequency range, (b) low-frequency response, (c) medium-frequency response, (d) high-frequency response.

The samples of the mass and stiffness matrices are simulated following the procedure outlined in the previous section.

6. Comparison: experimental results vs random matrix theory

In many situations, complete statistical information about the uncertainty in the system is scarce. We are particularly interested in such cases and adopted random matrix approach to investigate its usefulness and limitations to model uncertainty in the context of coupled plate-oscillator assembly. Specifically, the detailed statistics of FRFs, which are random functions in frequency, will be studied in a next step. The statistical characteristics of cross and direct FRFs obtained from the experiments and random matrix theory are compared. For each FRF, we study the statistics of both amplitude and phase spectra to contrast the predictive capability of random matrix method in relation to the experimental results. It is worthwhile to reiterate the fact that the random matrix approach uses only the limited statistical information necessary to calculate the dispersion parameters σ_G (see Eq. (18)). In this paper we will discuss the results corresponding to the driving-point FRF (point 1), one *near-field* cross-FRF (point 2) and one *far-field* cross-FRF (point 6) only. Results for three other points are not presented for brevity but can be obtained from the data shared on the world wide web.

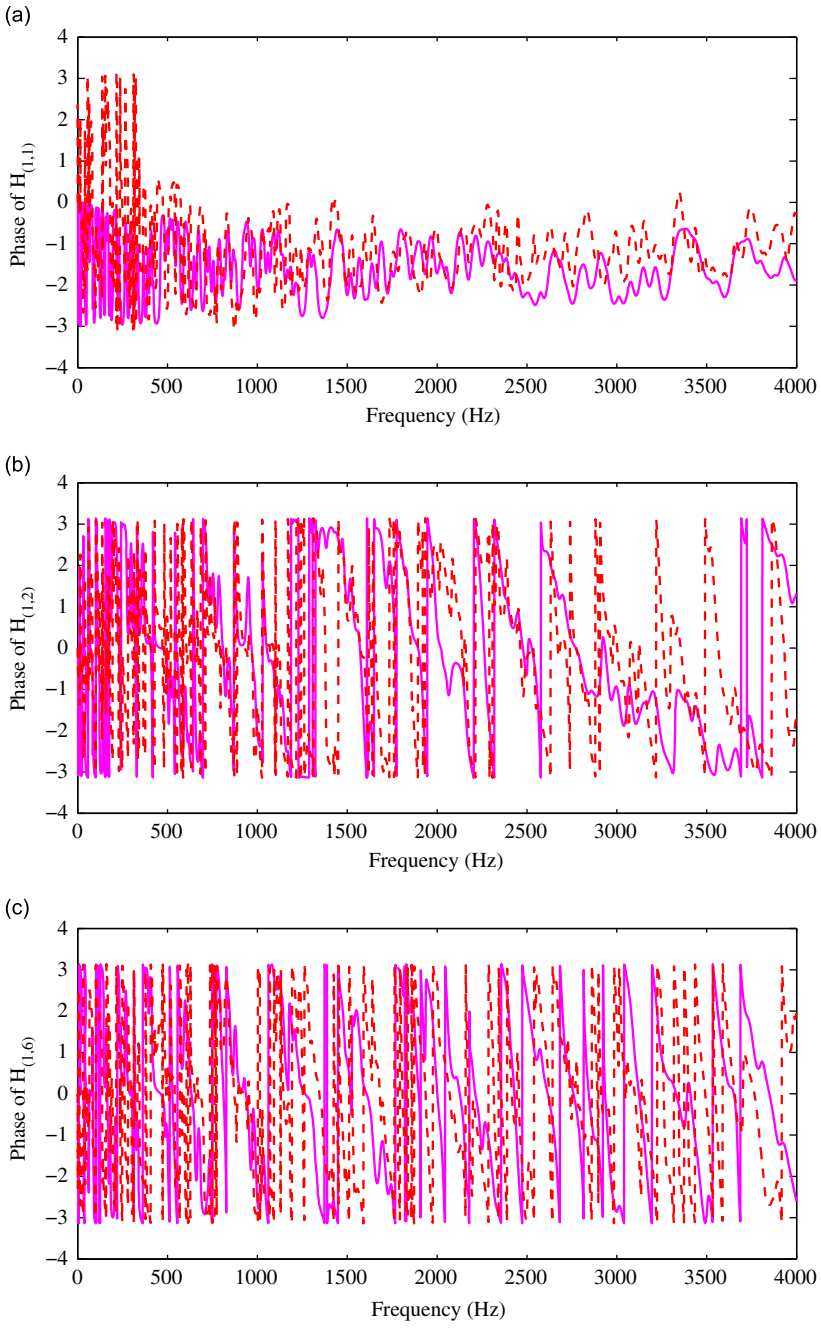

Fig. 11. Comparison of the phase of the FRF of the baseline system for the three selected points in the plate across the complete frequency range; – FE model; - - - experiment. (a) Driving-point FRF of the plate at point 1 (nodal coordinate: (4, 6)), (b) near-field cross-FRF of the plate at point 2 (nodal coordinate: (6, 11)), (c) far-field cross-FRF of the plate at point 6 (nodal coordinate: (21, 10)).

6.1. Amplitude spectra

First we compare the FRF of the baseline experimental system and the baseline FE model for the three points considered. In Fig. 7 the amplitudes of the FRF of the baseline system obtained using the deterministic FE model and experiment are compared. In general the experimental results and the finite element results are

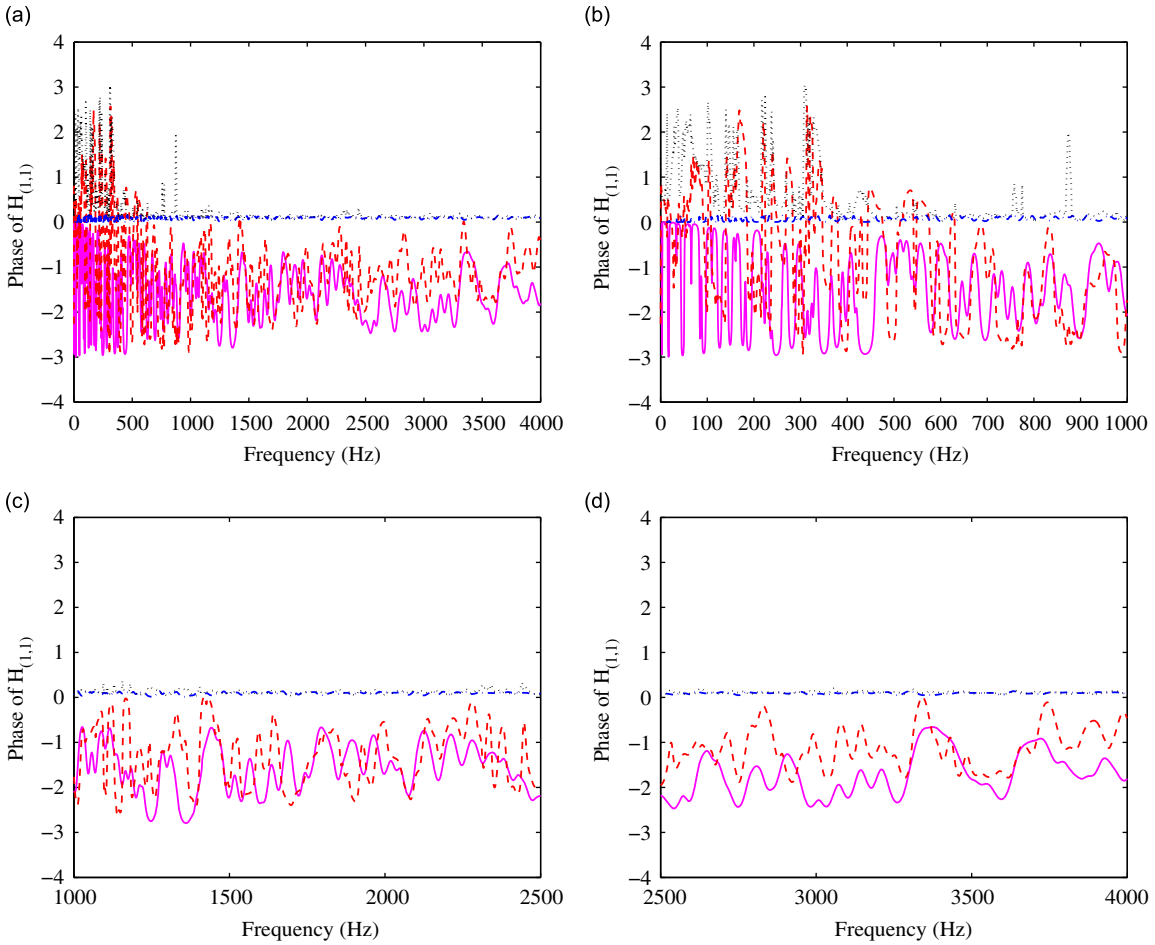

Fig. 12. Comparison of the mean and standard deviation of the phase of the driving-point FRF of the plate at point 1 (nodal coordinate: (4, 6)) with 10 randomly placed oscillators; — ensemble mean from Wishart model; - - - ensemble mean from experiment; -.-. standard deviation from Wishart model; ... standard deviation from experiment. (a) Response across the frequency range, (b) low-frequency response, (c) medium-frequency response, (d) high-frequency response.

within 10 dB. The main reason for the discrepancies is perhaps due to the use of constant modal damping factors for all modes in the FE model.

Next we compare the experimental results with the direct Monte Carlo simulation using random matrices. Fig. 8 compares the ensemble mean and standard deviation of the amplitude of the driving-point FRF at point 1 obtained from the experiment and Monte Carlo simulation. Figs. 8(b)–(d) show the low-, medium- and high-frequency response separately, obtained by zooming around the appropriate frequency ranges in Fig. 8(a). There are, of course, no fixed or definite boundaries between the low-, medium- and high-frequency ranges. We have selected $0-1.0$ kHz as the low-frequency vibration, $1.0-2.5$ kHz as the medium-frequency vibration and $2.5-4$ kHz as the high-frequency vibration. These frequency boundaries are selected on the basis of the qualitative nature of the response and devised purely for the presentation of the results. The experimental approach discussed is independent on these selections. The measured FRF data up to 4.0 kHz are significantly noise-free, since the hard steel tip used was able to excite the entire frequency range. The experimental data shown throughout the paper are the 'raw data' (that is, without any filtering) obtained directly from the LMS system. The standard deviation of the amplitude of the FRF reaches a peak at the system natural frequencies, which is also predicted by the numerical simulation. Qualitatively the simulation results agree well with the experimental results. The discrepancies, especially in the low frequency regions, are perhaps due to incorrect

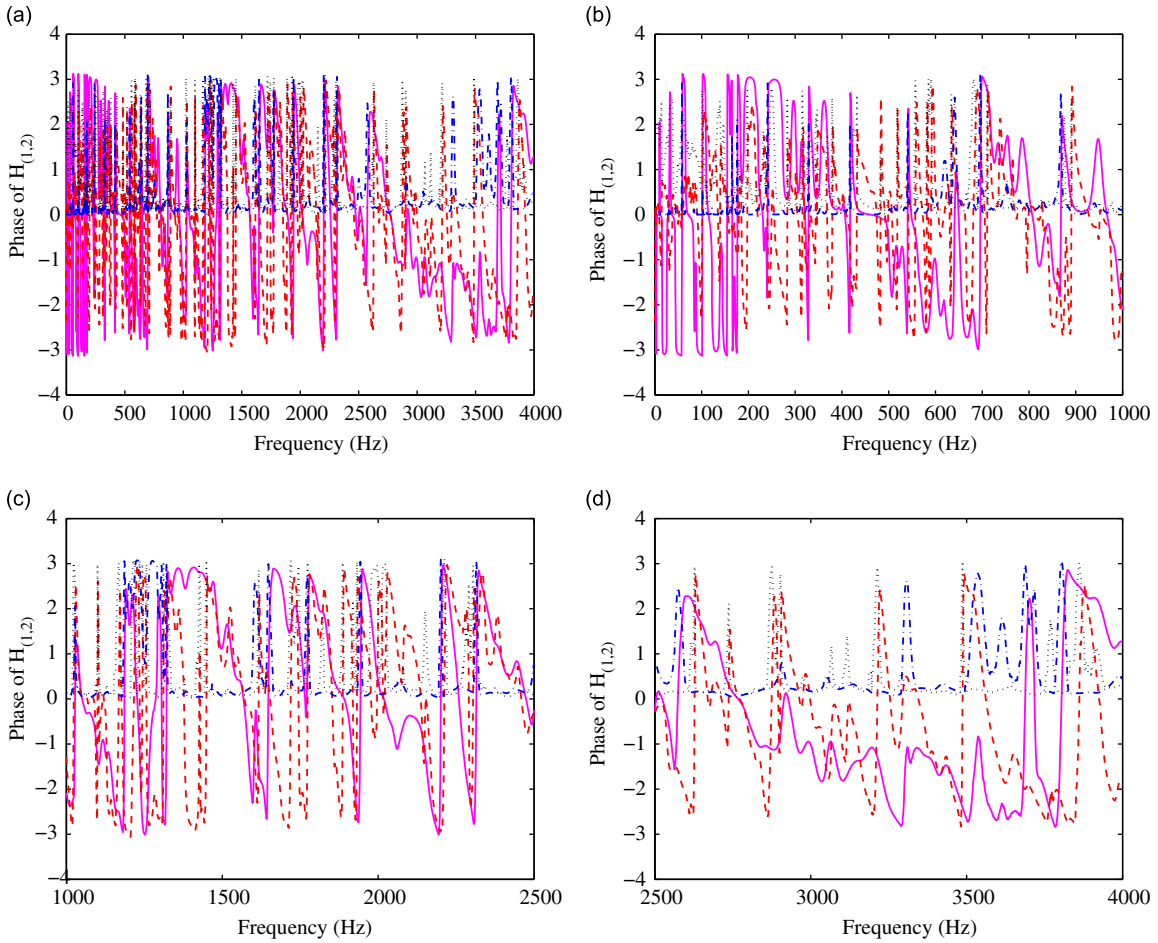

Fig. 13. Comparison of the mean and standard deviation of the phase of the near-field cross-FRF of the plate at point 2 (nodal coordinate: (6, 11)) with 10 randomly placed oscillators; — ensemble mean from Wishart model; - - - ensemble mean from experiment; -.-. standard deviation from Wishart model; ... standard deviation from experiment. (a) Response across the frequency range, (b) low-frequency response, (c) medium-frequency response, (d) high-frequency response.

values of the damping factors. In the simulation study a constant damping factor of 0.7% is assumed for all of the modes. Ideally one should estimate modal damping factors from experimental measurements for all of the samples and for as many modes as possible and perhaps take an average across the samples for every mode. Such extensive task is not undertaken here.

Equivalent comparisons for points 2 and 6 (a near and a far cross-FRF) are shown in Figs. 9 and 10. For all three points, the experimental mean and standard deviation in the low frequency range is quite high compared to numerical results. This may be attributed to the erroneous values of modal damping factors in the numerical model since the pattern of the peaks are strikingly similar but they are separated in 'height'. This is a clear indication that the damping values are incorrect in the simulation model. The study clearly demonstrates that the incorrect values of the modal damping factors can lead to significant errors in the predicted uncertainty using the proposed Wishart random matrices.

6.2. Phase spectra

First we compare the FRF of the baseline experimental system and baseline FE model for the three points considered. In Fig. 11 the phase of the FRF of the baseline system obtained using the deterministic FE model and experiment are compared.

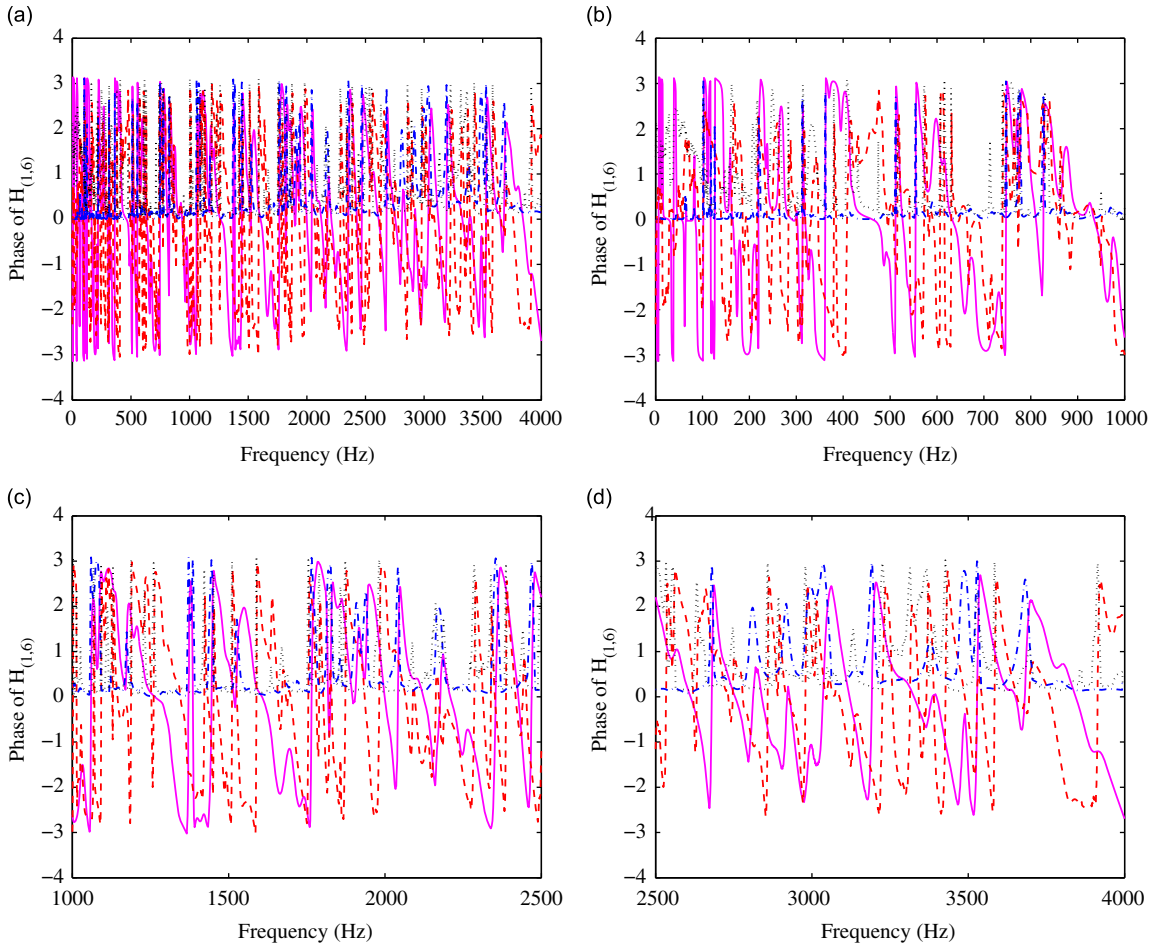

Fig. 14. Comparison of the mean and standard deviation of the phase of the far-field cross-FRF of the plate at point 6 (nodal coordinate: (21, 10)) with 10 randomly placed oscillators; — ensemble mean from Wishart model; - - - ensemble mean from experiment; -.-. standard deviation from Wishart model; ... standard deviation from experiment. (a) Response across the frequency range, (b) low-frequency response, (c) medium-frequency response, (d) high-frequency response.

Fig. 12 compares the ensemble mean and standard deviation of the phase of the driving-point FRF at point 1 obtained from the experiment and Wishart random matrix simulation. Figs. 12(b)–(d) show the low-, medium- and high-frequency response separately, obtained by zooming around the appropriate frequency ranges in Fig. 12(a). Except in the low frequency range, the standard deviation of the phase of the FRF is very small. The patterns of the mean results from the experiment and simulation are very similar across the frequency range. Again, the discrepancies are perhaps due to incorrect values of damping used in the numerical results.

Equivalent comparisons for points 2 and 6 (relating to the near-field and far-field cross-FRF) are shown in Fig. 13 and 14. The experimental mean in the mid- and high-frequency range is somewhat different from the random matrix simulations. Again, this is very likely to be due to inaccurate damping model. It is well-known that the damping has significant effect on the phase of the FRFs.

7. Conclusions

We attempted to describe model uncertainty in linear dynamical systems using random matrix theory. The feasibility of adopting Wishart random matrices to quantify uncertainty in the dynamical systems has been

explored using experimental data. In particular, model uncertainty in a vibrating plate due to disorderly attached sprung-mass oscillators with random natural frequencies is considered. One hundred nominally identical dynamical systems were statistically generated and individually tested in a laboratory setup. Special measures were taken so that the uncertainty in the response of the main structure primarily emerges from the random attachment configurations of the subsystems having random natural frequencies. Furthermore the experiments are repeatable with minimal changes. Novel measures to ensure these facts include (a) the use of a shaker as an impact hammer to induce a consistent force applied at a specific location for all tests, (b) the use of a hard steel tip to obtain relatively noise-free data up to 4 kHz, (c) the employment of a grid system and nodal points to minimize the error in measuring the oscillator and hammer locations, and (d) the use of magnets to attach the oscillators. The amplitude and phase of the measured FRFs at three different points in the plate are considered.

The agreement between the results obtained from the Wishart matrix model and physical experiments are encouraging. The main challenge in applying this method in practice is to obtain the normalized standard deviations corresponding to the system matrices. Further investigation involving more complex systems should be undertaken in order to be able to draw general conclusions regarding the applicability of the Wishart random matrix model to tackle model uncertainty. The current study provides impetus for future investigations along this direction.

Acknowledgements

S.A. acknowledges the financial support of the UK Engineering and Physical Sciences Research Council (EPSRC) through the award of an Advanced Research Fellowship and the Royal Society of London for the award of a visiting fellowship at Carleton University, Canada. A.S. acknowledges the support of a Discovery Grant from Natural Sciences and Engineering Research Council of Canada and the Canada Research Chair Program.

References

[1] F.M. Hemez, Y. Ben-Haim, The good, the bad, and the ugly of predictive science, in: K.M. Hanson, F.M. Hemez (Eds.), *Proceedings of the 4th International Conference on Sensitivity Analysis of Model Output*, Santa Fe, New Mexico, USA, 2004, pp. 181–193, see ⟨http://library.lanl.gov/⟩.

[2] M. Shinozuka, F. Yamazaki, Stochastic finite element analysis: an introduction, in: S.T. Ariaratnam, G.I. Schuëller, I. Elishakoff (Eds.), *Stochastic Structural Dynamics: Progress in Theory and Applications*, Elsevier Applied Science, London, 1998.

[3] R. Ghanem, P. Spanos, *Stochastic Finite Elements: A Spectral Approach*, Springer, New York, USA, 1991.

[4] M. Kleiber, T.D. Hien, *The Stochastic Finite Element Method*, Wiley, Chichester, 1992.

[5] H.G. Matthies, C.E. Brenner, C.G. Bucher, C.G. Soares, Uncertainties in probabilistic numerical analysis of structures and solids—stochastic finite elements, *Structural Safety* 19 (3) (1997) 283–336.

[6] C.S. Manohar, S. Adhikari, Dynamic stiffness of randomly parametered beams, *Probabilistic Engineering Mechanics* 13 (1) (1998) 39–51.

[7] S. Adhikari, C.S. Manohar, Dynamic analysis of framed structures with statistical uncertainties, *International Journal for Numerical Methods in Engineering* 44 (8) (1999) 1157–1178.

[8] S. Adhikari, C.S. Manohar, Transient dynamics of stochastically parametered beams, *ASCE Journal of Engineering Mechanics* 126 (11) (2000) 1131–1140.

[9] A. Sarkar, R. Ghanem, Mid-frequency structural dynamics with parameter uncertainty, *Computer Methods in Applied Mechanics and Engineering* 191 (47–48) (2002) 5499–5513.

[10] R. Ghanem, A. Sarkar, Reduced models for the medium-frequency dynamics of stochastic systems, *Journal of the Acoustical Society of America* 113 (2) (2003) 834–846.

[11] A. Sarkar, R. Ghanem, A substructure approach for the midfrequency vibration of stochastic systems, *Journal of the Acoustical Society of America* 113 (4) (2003) 1922–1934 (part 1).

[12] P.B. Nair, A.J. Keane, Stochastic reduced basis methods, *AIAA Journal* 40 (8) (2002) 1653–1664.

[13] I. Elishakoff, Y.J. Ren, *Large Variation Finite Element Method for Stochastic Problems*, Oxford University Press, Oxford, UK, 2003.

[14] S.K. Sachdeva, P.B. Nair, A.J. Keane, Comparative study of projection schemes for stochastic finite element analysis, *Computer Methods in Applied Mechanics and Engineering* 195 (19–22) (2006) 2371–2392.

[15] S.K. Sachdeva, P.B. Nair, A.J. Keane, Hybridization of stochastic reduced basis methods with polynomial chaos expansions, *Probabilistic Engineering Mechanics* 21 (2) (2006) 182–192.

[16] C. Soize, A model and numerical-method in the medium frequency-range for vibroacoustic predictions using the theory of structural fuzzy, *Journal of the Acoustical Society of America* 94 (2) (1993) 849–865 (part 1).
[17] M. Strasberg, D. Feit, Vibration damping of large structures induced by attached small resonant structures, *Journal of the Acoustical Society of America* 94 (3) (1995) 1814–1815.
[18] D.A. Russell, V.W. Sparrow, Backscattering from a baffled finite plate strip with fuzzy attachments, *Journal of the Acoustical Society of America* 98 (3) (1995) 1527–1533.
[19] R.L. Weaver, Mean and mean-square responses of a prototypical master/fuzzy structure, *Journal of the Acoustical Society of America* 101 (3) (1997) 1441–1449.
[20] O.C. Zienkiewicz, R.L. Taylor, *The Finite Element Method*, fourth ed., McGraw-Hill, London, 1991.
[21] C. Soize, A nonparametric model of random uncertainties for reduced matrix models in structural dynamics, *Probabilistic Engineering Mechanics* 15 (3) (2000) 277–294.
[22] C. Soize, Maximum entropy approach for modeling random uncertainties in transient elastodynamics, *Journal of the Acoustical Society of America* 109 (5) (2001) 1979–1996 (part 1).
[23] H. Chebli, C. Soize, Experimental validation of a nonparametric probabilistic model of nonhomogeneous uncertainties for dynamical systems, *Journal of the Acoustical Society of America* 115 (2) (2004) 697–705.
[24] C. Soize, Random matrix theory for modeling uncertainties in computational mechanics, *Computer Methods in Applied Mechanics and Engineering* 194 (12–16) (2005) 1333–1366.
[25] C. Soize, E. Capiez-Lernout, J.-F. Durand, C. Fernandez, L. Gagliardini, Probabilistic model identification of uncertainties in computational models for dynamical systems and experimental validation, *Computer Methods in Applied Mechanics and Engineering* 198 (1) (2009) 150–163.
[26] M.P. Mignolet, C. Soize, Nonparametric stochastic modeling of linear systems with prescribed variance of several natural frequencies, *Probabilistic Engineering Mechanics* 23 (2–3) (2008) 267–278.
[27] M.P. Mignolet, C. Soize, Stochastic reduced order models for uncertain geometrically nonlinear dynamical systems, *Computer Methods in Applied Mechanics and Engineering* 197 (45–48) (2008) 3951–3963.
[28] M.P. Mignolet, C. Soize, Nonparametric stochastic modeling of structures with uncertain boundary conditions and uncertain coupling between substructures, *Proceedings of the 49th Structures, Structural Dynamics, and Materials Conference* (SDM), American Institute of Aeronautics and Astronautics (AIAA), Schaumburg, Illinois, USA, 2008.
[29] M.P. Mignolet, P.C. Chen, Aeroelastic analyses with uncertainty in structural properties, *Proceeding of the AVT-147 Symposium: Computational Uncertainty in Military Vehicle Design*, Athens, Greece, 2007.
[30] M.P. Mignolet, C. Soize, K. Kim, D.H. Lee, Nonparametric stochastic modeling of structural dynamic and aeroelastic systems: formulation and novel extensions, *Proceedings of the 48th Structures, Structural Dynamics, and Materials Conference* (SDM), American Institute of Aeronautics and Astronautics (AIAA), Honolulu, Hawaii, 2007.
[31] M. Arnst, D. Clouteau, H. Chebli, R. Othman, G. Degrande, A non-parametric probabilistic model for ground-borne vibrations in buildings, *Probabilistic Engineering Mechanics* 21 (1) (2006) 18–34.
[32] S. Adhikari, Matrix variate distributions for probabilistic structural mechanics, *AIAA Journal* 45 (7) (2007) 1748–1762.
[33] S. Adhikari, On the quantification of damping model uncertainty, *Journal of Sound and Vibration* 305 (1–2) (2007) 153–171.
[34] S. Adhikari, Wishart random matrices in probabilistic structural mechanics, *ASCE Journal of Engineering Mechanics* 134 (12) (2008) 1029–1044.
[35] A. Gupta, D. Nagar, *Matrix Variate Distributions, Monographs & Surveys in Pure & Applied Mathematics*, Chapman & Hall, CRC, London, 2000.
[36] M.S. Kompella, B.J. Bernhard, Measurement of the statistical variations of structural-acoustics characteristics of automotive vehicles, *SAE Noise and Vibration Conference*, Society of Automotive Engineers, Warrendale, USA, 1993.
[37] F. Fahy, *Foundations of Engineering Acoustics*, Academic Press Inc., London, UK, 2000.
[38] M.I. Friswell, J.A. Coote, M.J. Terrell, S. Adhikari, J.R. Fonseca, N.A.J. Lieven, Experimental data for uncertainty quantification, *Proceedings of the 23rd International Modal Analysis Conference (IMAC-XXIII)*, Society of Experimental Mechanics (SEM), Orlando, FL, USA, 2005.
[39] C.S. Manohar, A.J. Keane, Statistics of energy flow in one dimensional subsystems, *Philosophical Transactions of Royal Society of London A* 346 (1994) 525–542.
[40] R.H. Lyon, R.G. Dejong, *Theory and Application of Statistical Energy Analysis*, second ed., Butterworth, Heinmann, Boston, 1995.
[41] R.S. Langley, P. Bremner, A hybrid method for the vibration analysis of complex structural-acoustic systems, *Journal of the Acoustical Society of America* 105 (3) (1999) 1657–1671.
[42] B.R. Mace, P.J. Shorter, Energy flow models from finite element analysis, *Journal of Sound and Vibration* 233 (3) (2000) 369–389.
[43] R.S. Langley, V. Cotoni, Response variance prediction for uncertain vibro-acoustic systems using a hybrid deterministic-statistical method, *Journal of the Acoustical Society of America* 122 (6) (2007) 3445–3463.
[44] V. Cotoni, P. Shorter, R.S. Langley, Numerical and experimental validation of a hybrid finite element-statistical energy analysis method, *Journal of the Acoustical Society of America* 122 (1) (2007) 259–270.
[45] Y. Lei, M.I. Friswell, S. Adhikari, A Galerkin method for distributed systems with non-local damping, *International Journal of Solids and Structures* 43 (11–12) (2006) 3381–3400 (among the top 25 most downloaded articles in April–June 2006).
[46] M.I. Friswell, S. Adhikari, Y. Lei, Vibration analysis of beams with non-local foundations using the finite element method, *International Journal for Numerical Methods in Engineering* 71 (11) (2007) 1365–1386.
[47] M.I. Friswell, S. Adhikari, Y. Lei, Nonlocal finite element analysis of damped beams, *International Journal of Solids and Structures* 44 (22–23) (2007) 7564–7576.

[48] A.M. Tulino, S. Verdú, *Random Matrix Theory and Wireless Communications*, Now Publishers Inc., Hanover, MA, USA, 2004.
[49] M.L. Eaton, *Multivariate Statistics: A Vector Space Approach*, Wiley, New York, 1983.
[50] R.J. Muirhead, *Aspects of Multivariate Statistical Theory*, Wiley, New York, USA, 1982.
[51] V.L. Girko, *Theory of Random Determinants*, Kluwer Academic Publishers, The Netherlands, 1990.
[52] M.I. Friswell, J.E. Mottershead, *Finite Element Model Updating in Structural Dynamics*, Kluwer Academic Publishers, The Netherlands, 1995.
[53] D.J. Ewins, *Modal Testing: Theory and Practice*, second ed., Research Studies Press, Baldock, England, 2000.
[54] N.M.M. Maia, J.M.M. Silva (Eds.), Theoretical and Experimental Modal Analysis, J.B. Robetrs (Eds.), *Engineering Dynamics Series*, Research Studies Press, Taunton, England, 1997.
[55] J.M.M. Silva, N.M.M. Maia (Eds.), *Modal Analysis and Testing: Proceedings of the NATO Advanced Study Institute*, NATO Science Series: E: Applied Science, Sesimbra, Portugal, 1998.
[56] A. Graham, *Kronecker Products and Matrix Calculus with Applications, Mathematics and its Applications*, Ellis Horwood Limited, Chichester, UK, 1981.